Chalcogenide Letters Vol. 12, No. 1, January 2015, p. 25 - 34

MICROWAVE PLASMA ASSISTED SULFURIZATION: A NEW APPROACH TO EFFECTIVELY PREVENT Sn LOSS IN Cu_2ZnSnS_4 FORMATION

T. CHEN*, Y. SUN
Institute of Photo-electronic Thin Film Devices and Technology ,Tianjin Key Laboratory of Thin Film Devices and Technology, Nankai University,Tianjin 300071, PR China

A new approach to prevent the loss of Sn element in Cu_2ZnSnS_4 sulfurization process, microwave plasma assisted sulfurization is developed, details of the specially designed microwave plasma sulfurization reactor is shown. Test of the reactor is performed in the sulfurization process of electrodeposited Cu/Sn/Zn precursors. XRF results indicate that no Sn loss is observed in the microwave plasma sulfurized samples, XRD analysis confirms no Sn loss in microwave plasma sulfurized sample with the Cu_4SnS_4 indicator theory. Further XRD, Raman and FESEM analysis is performed to demonstrate the temperature effects and other features of microwave plasma sulfurized samples. Microwave plasma sulfurization shows its effectiveness in preventing Sn loss in the Cu_2ZnSnS_4 formation.

(Received December 12, 2014; Accepted January 19, 2015)

Keywords: Microwave plasma, Sulfurization reactor, Sn loss, Cu_4SnS_4, Cu_2ZnSnS_4

1. Introduction

Earth-abundant Kesterite Cu_2ZnSnS_4 compound has its promising application in the low cost fabrication of thin film solar cells [1]. In the fabrication of Cu_2ZnSnS_4, most synthesis approaches employ the annealing of metallic precursor in a sulfur-containing environment, sulfur vapor obtained by evaporating solid sulfur is a safe and cost-effective way of sulfur provision in comparison with the toxic and explosive H_2S. However, in most sulfur vapor sulfurized films, a noticeable amount of Sn is lost due to the escape of gas phase SnS[2-5], which makes composition control very unstable.

In conventional vapor sulfurization, the evaporated sulfur vapor contains mostly S_8 rings instead of reactive sulfur dimmers(S_2), high concentration sulfur dimmer can only be generated at extremely high temperatures (>600℃ way above glass melting point) due to the high enthalpy of formation[6]. We think the presence of high concentration reactive sulfur dimmer is what will effectively prevent the loss of Sn. In order to crack the large chain S_8 molecules into reactive S_2 without using high temperature thermal decomposition, other decomposition pattern of S_8 chains should be considered.

Plasma seems to be a feasible way to crack large S_8 chains into reactive S_2, especially microwave plasma which is large-scale applicable[7], microwave plasma possesses so many unique properties such as high plasma density , no electrode contamination[8], these unique properties happens to be what is needed in the corrosive sulfurization environment. Actually, the new approach is inspired by the microwave sulfur lamp which is based on the molecular emission of S_2, S_8 rings is effectively and mostly cracked into S_2 by microwave radiation[9, 10], yet microwave plasma has not been applied in the sulfurization process of Cu_2ZnSnS_4 or other material sulfurization process.

* Corresponding author: taichen_nku@sina.com

In order to test if microwave plasma sulfurization is feasible, a microwave plasma sulfurization reactor is specially designed and made. This article demonstrates the details of the microwave plasma reactor, including several simple and effective engineering solutions to meet the demanding needs of sulfurization, inspired by basic physics principles. Electrodeposited Cu/Sn/Zn precursors are sulfurized, XRF, XRD, Raman and FESEM tests are performed to analyze the microwave plasma sulfurized samples. We hope that the reactor design and analysis of the new approach could be of some use to the future application of microwave plasma sulfurization in various cases requiring high density reactive S_2.

2. Microwave plasma sulfurization reactor:

To apply microwave plasma in the sulfurization process, a microwave plasma reactor needs to be specially designed in order to meet sulfurization needs. Several reactor engineering details are illustrated and explained below so that our work can be reproduced and confirmed.

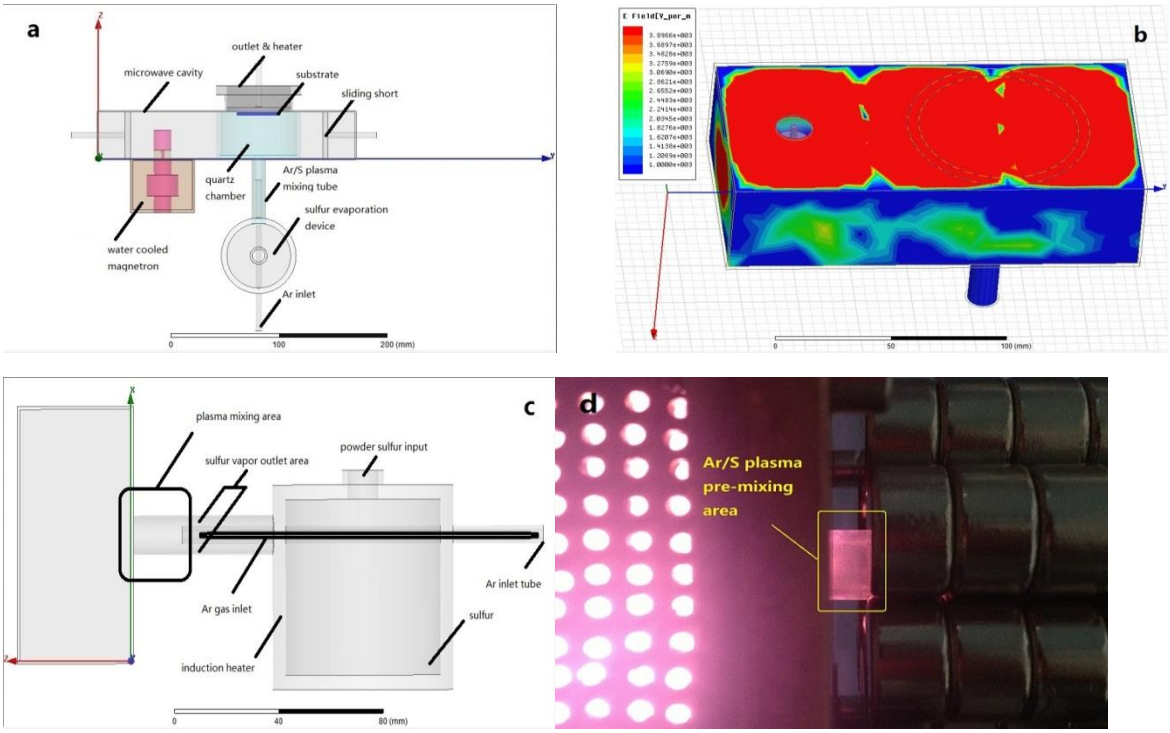

Fig. 1 (a) planar view of the schematic (b) HFSS simulation result of the cavity (c) schematic of sulfur source (d) plasma pre-mixing area

Fig. 1 (a) shows the schematic of the reactor. The Ar gas works as carrier gas and plasma ignition gas, sulfur vapor is provided after the Ar plasma is ignited. The substrate is exposed to the plasma, substrate heater is positioned at the back of the substrate. For contrast experiment, the reactor can function as a conventional two-zone sulfurization furnace[2] if the microwave is turned off. What needs to be emphasized is that the microwave cavity is based on a simple WR340 waveguide, unlike other complicated microwave plasma device, the plasma quartz chamber is positioned in the middle of two standing wave area instead of just one, this symmetrical position of the main chamber assists uniform plasma generation, the observed uniform plasma is shown in Fig.2 a and b.

Fig. 1 (b) shows the HFSS simulation result of the reactor, the intensity of the E field is strong and uniformly distributed, which is also another reason why we can obtain uniform plasma even in such small space. The outer diameter of the quartz chamber is 65 mm, the quartz thickness is 3mm. The microwave radiation is designed to leak out of the cavity through a 15mm diameter hole into the upper tube of quartz chamber, exactly where mixed sulfur vapor and Ar gas go through. The intensity of E in the upper tube reaches a level of e^{+3}, enough to sustain the plasma in the upper quartz tube without affecting the plasma stability and uniformity in the main quartz chamber(due to the symmetrical position). The purpose of this radiation leak design is to create a first stage plasma mixing area, further details is explained in Fig.1 (d).

Fig. 1 (c) shows the schematic of specially designed sulfur source. In the two zone sulfurization, S vapor is brought to the substrate by blowing the Ar gas across the sulfur evaporation surface, this will cause some side effects. When the Ar gas contacts the S evaporation surface directly, it will cool down the sulfur vapor, the cooling effect of carrier gas Ar could decrease the reactivity of sulfur vapor. To overcome this cooling, high temperature sulfur heating has to be applied to obtain a more reactive environment, however, as a result, a significant amount of sulfur is wasted due the condensation of excessive sulfur vapor generated by high temperature heating.

In our design, these problems can be avoided. As shown in (c), the Ar gas inlet pipe is positioned near the main chamber, outside of the evaporator bucket. As the vacuum pump starts evacuating, the Ar gas will go to the main chamber without contacting or cooling the sulfur evaporating surface, also the flow of the Ar lowers the pressure of sulfur outlet area, the sulfur vapor will be pulled out of the evaporator, thus the temperature of sulfur heating no longer needs to be high enough to overcome the imposed Ar pressure in order to create excessive sulfur vapor[3], the waste of sulfur can be avoided, we can lower the sulfur heating temperature and evaporation rate, and still acquire excessive S_2 from the sulfur source with the plasma premixing explained below. We have tested this sulfur source, when the Ar pressure is 30 Pa, the sulfur heating temperature is 140℃ (creating a vapor pressure no more than 15 Pa , lower than the Ar pressure), we observed uniform Ar and Ar/S plasma , as shown in Fig. 2 a and b, respectively. The uniform plasma indicates that our sulfur source and reactor is functional.

Fig. 1 (d) shows the picture of plasma pre-mixing area. As shown in the HFSS simulation results, the microwave radiation is designed to leak out of the main chamber through the 15mm diameter hole into the upper quartz inlet tube, plasma can be generated inside the upper quartz tube where S vapor and Ar gas both goes through. Have been tested, the plasma pre-mixing area proves to be very efficient in avoiding sulfur condensation, no sulfur condensation was observed in the plasma pre-mixing area or the quartz chamber. More importantly, the design helps the Ar/S mixture to be pre-cracked and mixed uniformly before they go into the main chamber.

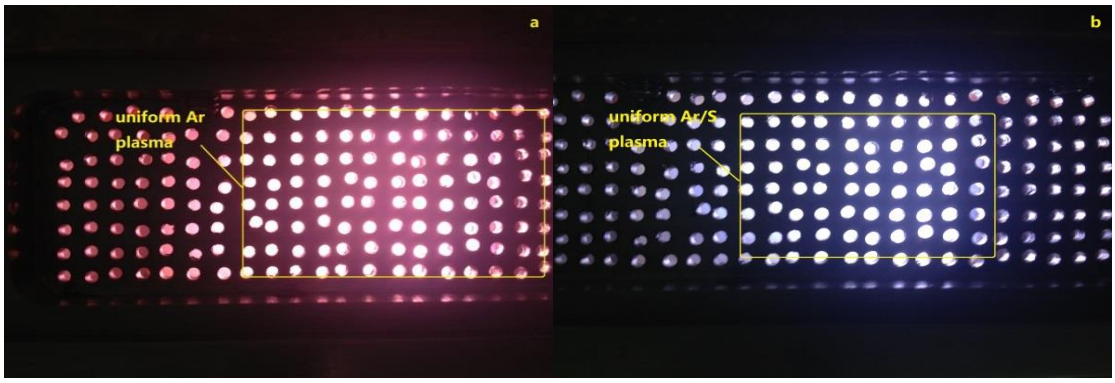

Fig.2. a. Ar plasma b. Ar/S plasma

3. Experiment

Table 1. Sulfurization and samples processing parameters

Microwave plasma sulfurization(*)			Non-plasma sulfurization(#)
Microwave power		200W	0W
Sulfur heating		140℃	300℃
Ar Flow rate		5sccm	5sccm
Pressure		30Pa	40Pa
Sample ID	Sulfurization Methods	Sulfurization Temperature	Sulfurization Time
A	*	350℃	20 min.
B	*	400℃	20 min.
C	*	450℃	20 min.
D	*	500℃	20 min.
γ	#	500℃	20 min.

The operating parameters of microwave plasma sulfurization and conventional non-plasma sulfurization are listed in the upper part of Table 1. With the typical parameters(*), no plasma etching to the substrate is observed throughout the testing of microwave plasma sulfurization reactor, The non-plasma sulfurization employs a sulfur heating temperature (300℃) higher than most of the reported ones[2, 5, 11].

The Non-plasma sulfurized sample γ is intended to make a contrast with the microwave plasma sulfurized sample D, this contrast experiment of γ and D (both substrate temperature 500℃) will demonstrate the difference between non-plasma sulfurization and the new microwave plasma sulfurization, especially the Sn loss condition, the effectiveness of the microwave plasma sulfurization in prevention of Sn loss can be established by this contrast experiment. We set the substrate temperature as the independent variable in the microwave plasma sulfurized samples (A,B,C,D), the plasma sulfurization parameter(*) and sulfurization time(20mins) is kept constant throughout the temperature dependent experiment.

The X-Ray fluorescence, (XRF-PANalytical) test is utilized to analyze the accurate composition of elements(1‰ accuracy ensured) in all samples before and after the microwave plasma sulfurization, the XRF test results will indicate if there are any Sn loss in the samples. The X-ray diffraction (XRD-PANalytical) test is performed to further back up the XRF test results, also demonstrates the temperature effect on the crystallinity of Cu_2ZnSnS_4. Raman spectra test (the wavelength is 785nm, a possible light penetration depth is 400nm [12]) is performed to confirm there is no existence of high temperature generated impurity phases in sample field rmission scanning electron microscopy FESEM (Hitachi) test which can demonstrate the surface and cross sectional image with high definition, is performed.

4. Results and discussion:

4.1 Confirming no loss of Sn via XRF test

Table 2.XRF test of samples before and after sulfurization

Sample ID	Chemical Composition (%) Before Sulfurization				Substrate Temp. (℃)	Chemical Composition (%) After Sulfurization					Sn Loss Condition Δ Sn / Cu
	Cu	Zn	Sn	Sn/Cu		Cu	Zn	Sn	S	Sn/Cu	
A	47.13	26.98	25.89	0.55	350*	36.54	20.93	20.06	22.47	0.55	0
B	47.25	26.04	26.71	0.57	400*	23.98	13.21	13.61	49.20	0.57	0
C	49.73	26.65	23.62	0.48	450*	24.31	13.05	11.62	51.02	0.48	0
D	48.81	26.92	24.27	0.50	500*	23.76	13.11	11.98	51.15	0.50	0
γ	46.95	26.76	26.29	0.56	500#	28.32	16.39	5.73	49.56	0.20	-0.36

Compositional data of samples before and after microwave plasma sulfurization is listed left and right in table 2, respectively, the Δ Sn / Cu is calculated to show the Sn loss condition in samples. A severe loss of Sn(Δ Sn / Cu=-0.36) is observed in sample γ, while no loss of Sn (Δ Sn / Cu=0) is observed in the microwave plasma sulfurized samples (A B C D), the mechanism that causes loss of Sn is discuss in 4.2 with details. The XRF test results shows that microwave plasma sulfurization is effective in preventing the loss of Sn.

4.2 Confirming no loss of Sn with XRD results

Listed in the Table 3 are five reactions that lead to the loss of Sn element by the escape of gas phase SnS, inspired by the equilibrium theory proposed by A. Redinger and S. Siebentritt[13], these undesired reactions can be interrupted if excessive product (SnS or S_2) is supplied, different from the compensation solution(providing gaseous SnS)of introducing elemental Sn in the presence of sulfur vapor, our approach is to generate high density S_2 via microwave plasma to drive the equilibrium of these undesired reactions to the reactant side, thus prevent the loss of Sn. Studying the equilibrium of undesired reactions could also provide us another point of view to see how the loss of Sn can be discovered.

Table 3. Reactions leading to Sn loss and their temperature range

No.	Reaction Equations	Temperature Range(℃)[12]
1	$4SnS_2(s) \rightarrow 2Sn_2S_3(s) + S_2(g)$	320 - 360
2	$2Sn_2S_3(s) \rightarrow 4SnS(g) + S_2(g)$	330 - 380
3	$4Cu_2SnS_3(s) \rightarrow 2Cu_4SnS_4(s) + 2SnS(g) + S_2(g)$	400 - 485
4	$2Cu_4SnS_4(s) \rightarrow 4Cu_2S(s) + 2SnS(g) + S_2(g)$	480 - 505
5	$2Cu_2ZnSnS_4(s) \rightarrow 2Cu_2S(s) + 2ZnS(s) + 2SnS(g) + S_2(g)$	480 - 505

If the undesired reactions start in sample γ (with sulfurization temperature 500℃ in the temperature range of reaction 4 and 5), the presence of Cu_4SnS_4 diffraction peaks can indicate that a certain amount of gas phase SnS has escaped. The presence of Cu_4SnS_4 in those Sn lost samples has been confirmed by R. Mainz and A. Webber in their in-situ XRD study of Cu-Sn-S system[12], based on their study and ours, we think that the existence of byproduct Cu_4SnS_4 from the undesired reactions should be considered as an indicator for Sn loss. Due to the existence of a strong molybdenum diffraction peak in the XRD patterns, most weak peaks are unclear if using the ordinary wide-ranging intensity scales. Scientifically speaking, logarithmic scales of the XRD intensity is an accurate way of demonstrating non-negligible weak peaks, so logarithmic scales is applied in all the XRD patterns shown in Fig.3.

However, the presence of Cu_2S and should not be used as an Sn loss indicator, because the Cu_2S could be generated by the decomposition of CuS (starts at the temperature of 350℃)[12]before the temperature reaches 500℃, this mechanism is confirmed by the Cu_2S presence (Fig.3 A & B) in our low temperature sulfurized sample A and B(both Δ Sn / Cu=0). ZnS should not be used as an indicator, either. Because the incomplete reaction (due to low temperature) between Cu_2SnS_3 and ZnS could leave a certain amount of residual ZnS, this is confirmed by the presence of some residual ZnS in our low temperature sulfurized sample A and B(Fig.3 A & B). The Sn_2S_3 and SnS exist only under low temperature (< 400℃[12]) , thus we do not use them as indicators for sample γ and D ,however, we indeed see no peaks of Sn_2S_3 and SnS in sample A and B(both Δ Sn / Cu=0).

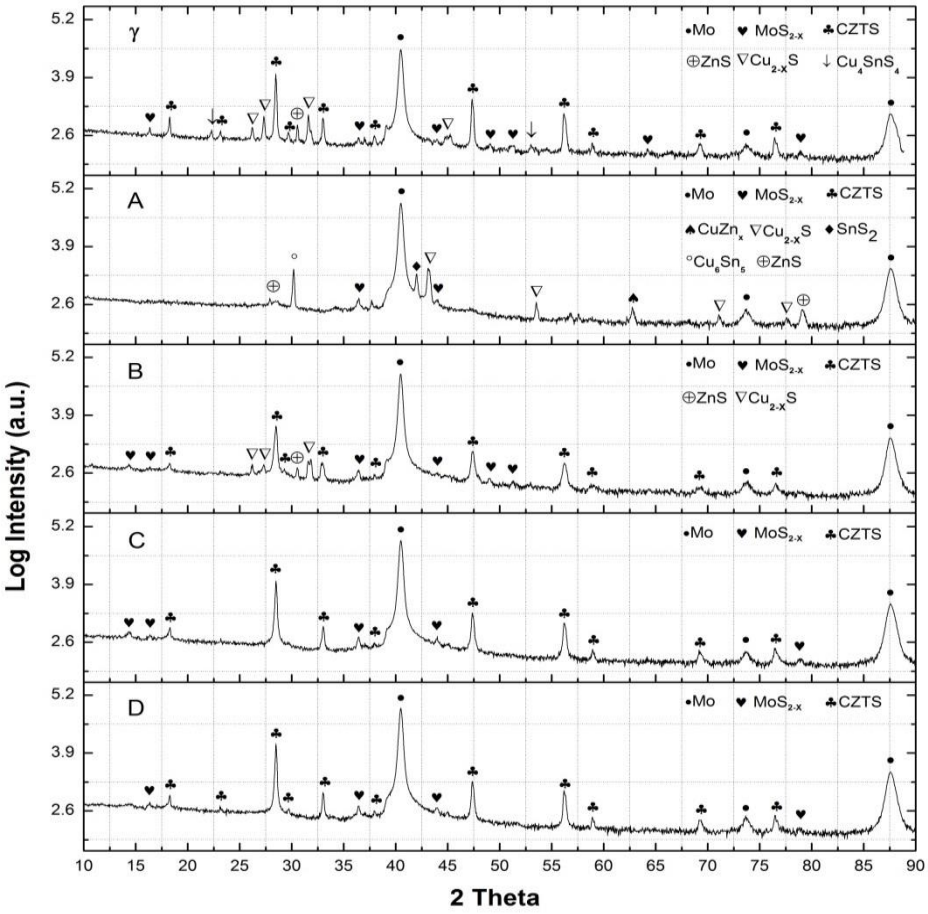

Fig.3. XRD patterns of samples

As we can see from Fig.3 γ and D , clear diffraction peaks of Cu_4SnS_4 is observed in sample γ, indicating the Sn loss reaction 3 has taken place, along with the severe Sn loss in sample γ, other undesired impurity phases ($Cu_{2-X}S$,ZnS) emerge, suggesting that Sn loss could bring potential bad crystallinity. No Cu_4SnS_4 peaks is observed in the sample D, which means no undesired reaction has taken place, thus no Sn is lost in microwave plasma sulfurized sample D. The XRD analysis of γ and D well support the Cu_4SnS_4 indicator theory and the XRF test results.

4.3 Further XRD, RAMAN and SEM test results analysis:

In sample A, diffraction peaks of $CuZn_x$ and Cu_6Sn_5 alloys are observed, also some binary sulfides ($Cu_{2-X}S$,SnS_2,ZnS).Diffraction peaks of Cu_2ZnSnS_4 is not found, this is because formation of Cu_2ZnSnS_4 does not start at 350℃ , as the temperature rises to 400℃ , diffraction peaks of Cu_2ZnSnS_4 can be found in sample B, but at 400℃ ,the transformation from sulfides to Cu_2ZnSnS_4 is not complete, as seen in XRD pattern of B, Cu_2ZnSnS_4 peak is very weak. As the temperature

rises to 450℃(sample C),stronger dominant Cu_2ZnSnS_4 diffraction peak(2θ=28.482°) is observed with no binary sulfides diffraction peaks found, indicating that all binary sulfides has been consumed by the formation reaction of Cu_2ZnSnS_4, the intensity of dominant Cu_2ZnSnS_4 diffraction peak in sample D increased due to a higher substrate temperature(500℃). It can be concluded that crystallinity of Cu_2ZnSnS_4 can be improved by elevating the substrate temperature.

Good crystallinity can be achieved by elevated substrate temperature[2], but secondary phases such as ZnS and Cu_2SnS_3 could be present due to the high temperature decomposition of Cu_2ZnSnS_4. The unit cell size of ZnS and Cu_2SnS_3 are similar to the one of Cu_2ZnSnS_4, making XRD identification of these secondary phases difficult if the Cu_2ZnSnS_4 dominant diffraction peak is present[14]. So a Raman test of sample D is performed. Shown in Fig.4, peaks of Cu_2ZnSnS_4 ($288cm^{-1}$,$336cm^{-1}$,$370cm^{-1}$) is observed with no fingerprints of ZnS ($275cm^{-1}$,$350cm^{-1}$) or Cu_2SnS_3 ($302cm^{-1}$,$354cm^{-1}$), peak identification is based on reported data[14], the Raman results shows there are no secondary phases in microwave plasma sulfurized sample D.

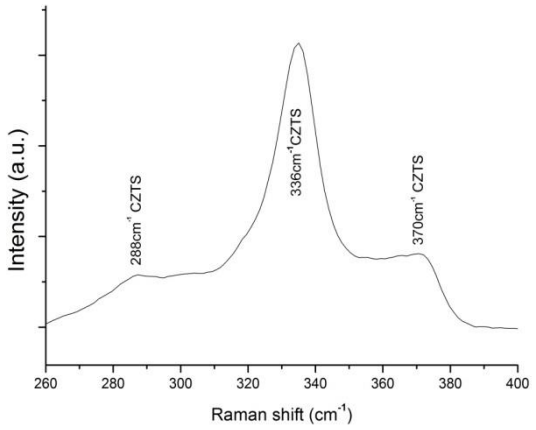

Fig.4. Raman spectra of sample D

The FESEM images of sample D and γ is shown in Fig.5. and Fig.6 , respectively. It has been suggested that the loss of Sn element could generate large porous region at the interface[15]. It is obvious when comparing the cross-sectional image of γ and D, without plasma sulfurization, the loss of Sn somehow generates a lot of voids in sample γ, the voids also results in a bad adhesion between the Cu_2ZnSnS_4 and the Mo, The surface of sample γ is attached strange shaped tiny grain which is probably the Cu_xS_y. The surface and cross-sectional image of sample D shows no voids, nor impurity grains attached to the surface, and the grain size is bigger than the one in sample γ, this is probably attributed to the prevention of Sn loss. Thus we think, by preventing the loss of Sn, surface morphology and crystal growth can be improved.

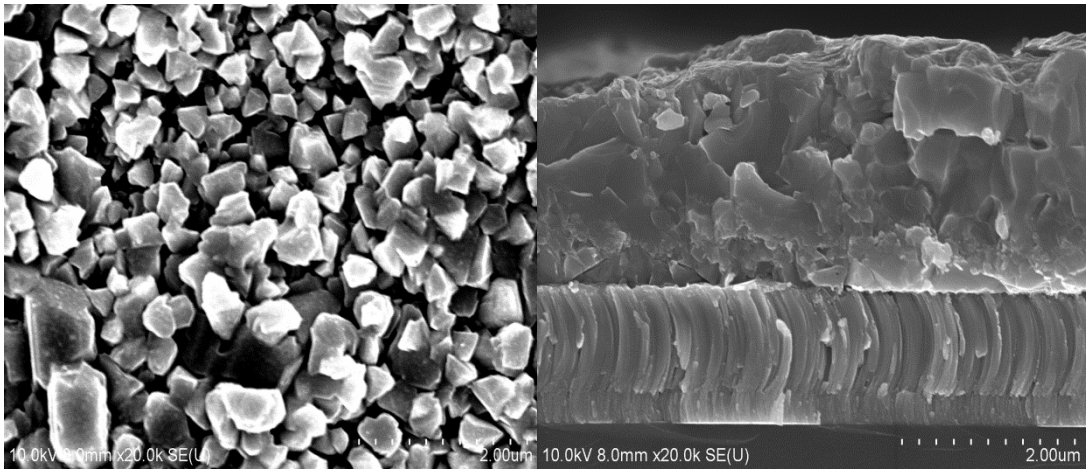

Fig.5 FESEM images of sample D

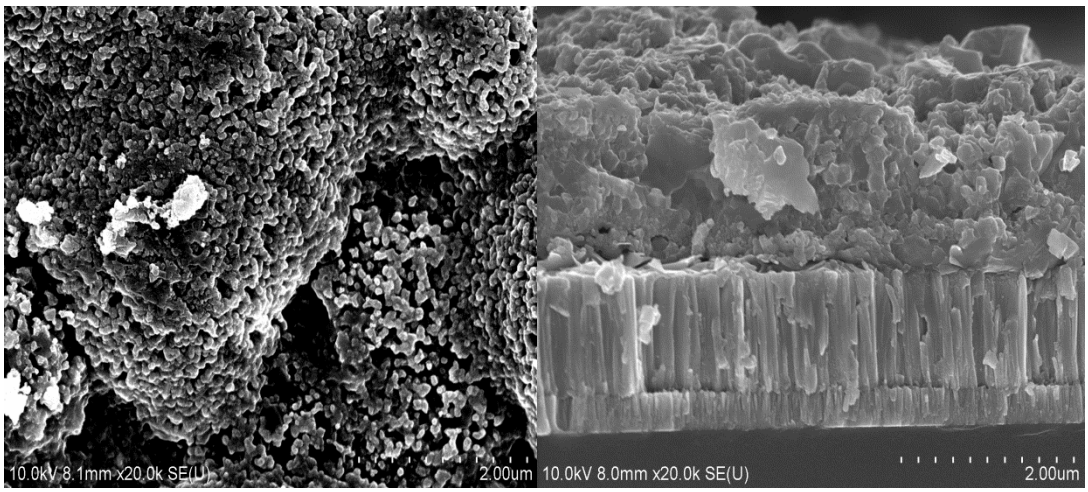

Fig.6. FESEM images of sample γ

5. Conclusion

The microwave plasma sulfurization reactor functions well in the sulfurization of electro-plated Cu-Sn-Zn precursors, XRF test results shows that there are no loss of Sn in the microwave plasma sulfurized samples, the XRD results further confirms this point with our Cu_4SnS_4 indicator theory, Raman results shows that there is no secondary phases such as Cu_2SnS_3 and ZnS in sample D, FESEM test also demonstrates that microwave plasma sulfurized samples do not have voids or impure grains, microwave plasma sulfurization shows its effectiveness in the prevention of Sn loss.

Reference

[1] H. Katagiri, K. Jimbo, W. S. Maw, K. Oishi, M. Yamazaki, H. Araki, A. Takeuchi, Thin Solid Films, **517**, 2455 (2009).

[2] H. Yoo, J. Kim, and L. Zhang, Current Applied Physics, **12**, 1052 (2012).

[3] E. M. Mkawi, K. Ibrahim, M. K. M. Ali, M. A. Farrukh, A. S. Mohamed, Journal of Materials Science: Materials in Electronics, **25**, 857 (2013).
[4] M. I. Amal, K. H. Kim, Journal of the Korean Physical Society, **63**, 2194 (2013).
[5] M. I. Amal, K. H. Kim, Thin Solid Films, **534**, 144 (2013).
[6] B. E. A. J. H. J. A. d. Keizer, W. E. K. I. K. R. S. Y. Steudel, M. W. Wong, Topics in Current Chemistry, pp. 117-134, 2003.
[7] M. Kaiser, K. M. Baumgärtner, A. Schulz, M. Walker, E. Räuchle, Surface and Coatings Technology, 116, 552 (1999).
[8] A. J. L. Michael A. Lieberman, "Principles of Plasma Discharges and Materials Processing, 2nd Edition," 2005.
[9] C. W. Johnston, J. Jonkers, J. J. A. M. Van Der Mullen, Journal of Physics D: Applied Physics, **35**, 2578 (2002).
[10] C. W. Johnston, H. W. P. Van Der Heijden, G. M. Janssen, J. Van Dijk, J. J. A. M. Van Der Mullen, Journal of Physics D: Applied Physics, **35**, 342 (2002).
[11] P. A. Fernandes, P. M. P. Salomé, A. F. da Cunha, Thin Solid Films, **517**, 2519 (2009).
[12] A. Weber, R. Mainz, H. W. Schock, Journal of Applied Physics, **107**, 013516 (2010).
[13] A. Redinger, D. M. Berg, P. J. Dale, S. Siebentritt, Journal of the American Chemical Society, **133**, 3320 (2011).
[14] P. A. Fernandes, P. M. P. Salomé, A. F. da Cunha, Journal of Alloys and Compounds, **509**, 7600 (2011).
[15] M. Oh, W. K. Kim, Journal of Alloys and Compounds, **616**, 436 (2014).